Chemico-Biological Interactions 229 (2015) 64–72

Contents lists available at ScienceDirect

Chemico-Biological Interactions

journal homepage: www.elsevier.com/locate/chembioint

Anti-thyroid and antifungal activities, BSA interaction and acid phosphatase inhibition of methimazole copper(II) complexes

Nora M. Urquiza [a], María S. Islas [b], Santiago T. Ariza [b], Nadir Jori [b], Juan J. Martínez Medina [c], Martín J. Lavecchia [d], Leonor L. López Tévez [c], Luis Lezama [e], Teófilo Rojo [e], Patricia A.M. Williams [b], Evelina G. Ferrer [b,*]

[a] Cátedra de Química Analítica, Instituto de Química Analítica, Facultad de Bioquímica, Química y Farmacia, Universidad Nacional de Tucumán, Ayacucho 471, 4000 San Miguel de Tucumán, Argentina
[b] Centro de Química Inorgánica (CEQUINOR/CONICET, UNLP), Facultad de Ciencias Exactas, UNLP, C. Correo 962, 1900 La Plata, Argentina
[c] Universidad Nacional del Chaco Austral, Cte. Fernández 755, 3700 Roque Sáenz Peña, Chaco, Argentina
[d] Instituto de Investigación Biomedicina de Buenos Aires (IBioBA)-CONICET-Partner Institute of the Max Planck Society, Godoy Cruz 2390, C1425FQA Buenos Aires, Argentina
[e] Departamento de Química Inorgánica, Facultad de Ciencia y Tecnología, Universidad del País Vasco, Apdo 644, 48080 Bilbao, Spain

ARTICLE INFO

Article history:
Received 13 June 2014
Received in revised form 9 December 2014
Accepted 31 December 2014
Available online 29 January 2015

Keywords:
Methimazole
Phenanthroline
Copper(II)
Antifungal activity
Anti-thyroid activity
BSA interactions

ABSTRACT

It has been reported that various metal coordination compounds have improved some biological properties. A high activity of acid phosphatase (AcP) is associated to several diseases (osteoporosis, Alzheimer's, prostate cancer, among others) and makes it a target for the development of new potential inhibitors. Anti-thyroid agents have disadvantageous side effects and the scarcity of medicines in this area motivated many researchers to synthesize new ones. Several copper(II) complexes have shown antifungal activities. In this work we presented for a first time the inhibition of AcP and the anti-thyroid activity produced by methimazole–Cu(II) complexes. Cu–Met ($[Cu(MeimzH)_2(H_2O)_2](NO_3)_2{\cdot}H_2O$) produces a weak inhibition action while Cu–Met–phen ($[Cu(MeimzH)_2(phen)(H_2O)_2]Cl_2$) shows a strong inhibition effect (IC_{50} = 300 μM) being more effective than the reported behavior of vanadium complexes. Cu–Met–phen also presented a fairly good anti-thyroid activity with a formation constant value, $K_c = 1.02 \times 10^{10}\ M^{-1}$ being 10^6 times more active than methimazole ($K_c = 4.16 \times 10^4\ M^{-1}$) in opposition to Cu–Met which presented activity ($K_c = 9.54 \times 10^3\ M^{-1}$) but in a lesser extent than that of the free ligand. None of the complexes show antifungal activity except Cu–phen (MIC = 11.71 μg mL^{-1} on *Candida albicans*) which was tested for comparison. Besides, albumin interaction experiments denoted high affinity toward the complexes and the calculated binding constants indicate reversible binding to the protein.

1. Introduction

In recent years, the study of enzyme inhibition mediated by coordination metal compounds has significantly increased as a consequence of the development of the applications of these compounds in medicine. A variety of metal complexes have been studied for this purpose including, complexes of Au(I), Pt(II), V(IV)O [1,2] and Cu(II) [3]. Recently, it has been demonstrated that copper(II) complexes acted as inhibitors of the protein tyrosine phosphatase (PTP) [4] and the alkaline phosphatase (ALP) enzyme [5,6].

On the other hand, purples acid phosphatases (PAP) are metalloenzymes found in animals, plants and fungi. These phosphatases have a binuclear structure with two different metal centers for the catalytic reaction of the hydrolysis of phosphate esters and anhydrides under acidic conditions (one is Fe(III) and the second one could be Fe(II) (in mammals) [7], or Zn(II) or Mn(II) (in plants) [8]). Basically, the structure and the mechanism of action are similar to that of alkaline phosphatase (ALP) and the difference would be the presence of a serine (Ser) amino acid residue [9] whereas in PAP a histidine (His) residue is present. Different biological roles have been proposed for PAP (iron transport during gestation, bone resorption in osteoclasts, catalysis of Fenton's reaction, etc) [10] and its elevated levels in serum are correlated with the progression of osteoporosis (bone metastases), Guacher and Alzheimer's diseases, hyperparathyroidism and prostate cancer, among others [11–13]. The activity of phosphatase acid could be inhibited by certain metal ions such as Hg(II), Cr(VI), Bi(III) [14], Cd (II) [15], some oxo-anions as $HAsO_4^{-2}$, WO_4^{-2} and MoO_4^{-2} [16], some organic

* Corresponding author. Tel./fax: +54 0221 4259485.
E-mail address: evelina@quimica.unlp.edu.ar (E.G. Ferrer).

http://dx.doi.org/10.1016/j.cbi.2014.12.036
0009-2797/

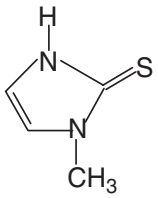

Fig. 1. Chemical structure of methimazole.

compounds [17] but there is not sufficient evidence in the literature concerning to the inhibitory tests performed with coordination compounds and we only found some studies for vanadium compounds [18]. Taking into account that high levels of this enzyme are associated with numerous diseases it turns out to be a good target for the development of new potential inhibitors.

In addition to the possibility of enzymatic inhibition, it is well known that methimazole (Fig. 1) is an anti-thyroid agent which most important effect is the inhibition of the thyroid hormone synthesis by interfering with thyroid peroxidase-mediated iodination of tyrosine residues in thyroglobulin (an important step in the synthesis of thyroxine and triiodothyronine). Disadvantageous side effects related with the drugs have been detected during the past years [19] inspiring researchers to synthesize new anti-thyroid agents with lesser side effects. However, no studies were found concerning the anti-thyroid effects of metal complexes. In consequence we decide to simulate *in vitro* the action of the present copper(II)-methimazole complexes as anti-thyroid drugs [20,21].

In recent years coordination complexes have been studied because of their potential biological applications. It has been revealed in many cases, an improvement of the activity. For this reason, we presented in this work, for a first time, the inhibition acid phosphatase studies and anti-tyroid activity of methimazole copper complexes. We also determined its antifungal and the albumin transport abilities. As it is known, serum albumin is the major transporter protein for unesterified fatty acids and also is capable to bind an extraordinarily diverse range of metabolites, drugs, dyes and organic compounds. Because the metabolism, distribution and efficacy of many drugs in the body are associated with their affinities towards serum albumin, the analysis of compounds with respect to albumin binding ability becomes a relevant item to analyze.

2. Materials and methods

2.1. Reagents and instrumentation

All chemicals were of analytical grade. Bovine Serum Albumin BSA (A-6003, essentially fatty acid-free) and acid phosphatase AcP (from potato, 0.8 U/mg, Deisenhofen, product number P-3752) were obtained from Sigma Chemical Company (St. Louis, MO) and used as supplied. Copper(II) nitrate trihydrate and Copper(II) chloride dihydrate were obtained from Merck. Methimazole, 1,10-phenanthroline monohydrate, para-nitrophenyl phosphate (p-NPP) and all the other analytical grade chemicals used were purchased from Sigma. Methimazol (MeimzH)–copper(II) complexes ($[Cu(MeimzH)_2(H_2O)_2](NO_3)_2{\cdot}H_2O$ (Cu–Met) and $[Cu(MeimzH)_2(phen)(H_2O)_2]Cl_2$ (Cu–Met–phen) and $[Cu(phen)_2Cl]Cl{\cdot}H_2O$ (Cu–phen) were prepared and purified according to published procedures [5,6].

2.2. Acid phosphatase inhibition test

Acid phosphatase inhibition test was performed according to Blum and Schwedt procedures [14]. Acetate buffer was prepared by dissolving a volume of 5.72 mL of concentrated acetic acid in distilled water (final volume of 250 mL) adjusting the pH to 5.60 with 0.5 M NaOH. The stock solution of the enzyme was made by mixing 12.5 mg of the 0.25 U/mL acid phosphatase powder in 2.0 ml acetate buffer. For use, 100 μL of the stock solution was diluted with 1.9 mL acetate buffer. For the substrate solution 0.170 g of p-NPP were dissolved in 2.5 mL distilled water.

2.2.1. Test procedure

The compounds solutions were prepared by diluting the stock solutions prepared in DMSO with acetate buffer. A volume of 0.50 mL of complex solution was mixed with 0.10 mL of the enzyme solution and 1.00 mL of buffer. The mixture was kept at 25 °C for 20 min (incubation time). After starting the reaction by adding 0.10 mL of the substrate solution, the tube was kept at 25 °C for 20 min. The reaction was stopped with the addition of 0.50 mL of a 0.5 M sodium hydroxide solution. The final concentration of DMSO resulted in 1.14%. The enzymatic activity was finally calculated by measuring the absorbance of 4-nitrophenolate at 405 nm against a blank prepared without the enzyme. Three independent replicates of each point were measured. The 100% of the enzyme activity is assigned to a basal measurement containing all the reaction media including the same volume of DMSO in all the experiments. It is worthy to mention that the presence of 1.14% DMSO did not affect the enzyme activity.

2.3. Anti-thyroid activity

Iodine was obtained from Merck. It was bisublimed and was kept in dark in a desiccator containing P_2O_5. Solvents used were bidistilled water and ethanol. Solutions of iodine and methimazole, o-phenanthroline, Cu–Met and Cu–Met–phen were prepared just before the beginning of experimentation. Stock solutions: iodine was always dissolved in ethanol while the compounds were dissolved in water. Iodine concentration was kept constant (4×10^{-4} M), though the concentration of the compounds was varied between 7×10^{-4} and 0.5×10^{-4} M. The reaction was carried out directly in the spectrophotometric cell by mixing 1.5 mL of each of compound (donor) and iodine (acceptor). Spectra were recorded immediately on double beam UV–visible spectrophotometer. The temperature of the solutions was kept at $25^0 \pm 1$ °C during the measurements. Three independent replicates of each solution were measured. Formation constant (K_c) and the molar extinction coefficient were determined using Lang's method [22]. This method has been used to determine the formation constants of 1:1 stoichiometric complexes at the wavelength under analysis using Eq. (1):

$$[A_0][D_0]/d_c = ([A_0] + [D_0] - d_c/\varepsilon_c)/\varepsilon_c + 1/K_c\varepsilon_c \quad (1)$$

in which, d_c is the absorbance, ε_c is the molar extinction coefficient and K_c is the formation constant of the complex. The Parameters were adjusted with a program designed by our research group.

Eq. (1) can be re-written in the form:

$$Y = (1/\varepsilon_c)X + 1/K_c\varepsilon_c \quad (2)$$

where $Y = [A_0][D_0]/d_c$ and $X = [A_0] + [D_0] - d_c/\varepsilon_c$.

From Eq. (2) a straight line with slope $1/\varepsilon_c$ and Y-intercept $1/(K_c\varepsilon_c)$ was obtained. Iteration and linear regression method were used to solve this equation.

2.4. Antifungal activity and post-antifungal effect (PAFE)

Antifungal activity was evaluated by the determination of the lowest concentration of the antimicrobial agent that inhibits the growth of fungus (minimum inhibitory concentration (MIC)) on three strains: *Candida parapsilosis* ATCC 22019, *Candida tropicalis* and *Candida albicans* of clinical isolates. The procedure was

performed according to our previous reported techniques [23]. In these experiments aqueous solutions of the metal salt ($CuCl_2{\cdot}2H_2O$) and the ligands were prepared and the Cu(II) complexes were dissolved in DMSO. An agar plate without anti fungus agent and containing the same volume of DMSO was established as a sterility and organism growth controls. It could be established that in our experimental conditions the bacterial strains were not affected by small aliquots of DMSO added to the cultures (the final concentration of DMSO resulted in 1.14%).

The post-antifungal effect (PAFE) is the time in which the antifungal agent was capable of causing growth suppression of the organism following limited tested agents' exposure [23]. In this study, the PAFEs were determined after the exposure of the fungal strains at twice the MIC (2 × MIC) value of phen and the complex Cu–phen, both dissolved in water and sterilized by filtration, for 1 h at 37 °C. The point at which microbial growth occurred was measured using a spectrophotometric method. Each PAFE measurement was carried out in triplicate. Details of the experimental procedure can be found in previous communications [23].

2.5. Interaction of the metal complex with bovine serum albumin

2.5.1. Binding affinity by fluorescence spectroscopy

BSA was dissolved in Tris–HCl (0.1 M, pH 7.4) buffer to attain a final concentration of 4% w/v (~0.6 mM). Phen, Cu–phen and Cu–Met–phen solutions were added dropwise to the 2% w/v BSA solution (~0.3 mM) to ensure the formation of a homogeneous solution and to obtain the desired concentration of 0.05–0.50 mM. Adequate solubility was reached under these experimental conditions in which the compounds did not show any fluorescence intensity that could interfere with the measurements. For each sample and concentration, three independent replicates were performed. These solutions were used for fluorescence measurements, which were carried out on a Perkin–Elmer LS-50B luminescence spectrometer (Beaconsfield, England) equipped with a pulsed xenon lamp (half peak height < 10 l s, 60 Hz), an R928 photomultiplier tube and a computer working with FL Winlab software. Both excitation and emission slits were set at 5 nm throughout this study. BSA 2% w/v was titrated by successive additions of phen, Cu–phen and Cu–Met–phen solutions from 0.05 to 0.50 mM and the fluorescence intensity was measured (excitation at 280 nm and emission at 348 nm) at 25 °C. All the fluorescence quenching data were analyzed according to previous studies performed in our laboratory applying the well-known Stern–Volmer equation and others traditional mathematical procedures [24,25] were applied to obtain the Stern–Volmer quenching constant and the binding constant (K_a) and the binding site value (n).

2.5.2. Conformation changes on protein structure after interaction with the metal complex: investigation by UV–vis and vibrational spectroscopies

FT-IR spectra of the freeze-dried powdered samples were measured with a Bruker IFS 66 FT-IR-spectrophotometer from 4000 to 400 cm^{-1} in the form of pressed KBr pellets. For data processing, spectra of the buffer were collected under the same conditions. Then, the spectrum of the buffer was subtracted from those of the samples to get the FT-IR spectra of the modified proteins. Thermoscientific DXR Smart Raman instrument equipped with CCD detector at a resolution between 2.7 and 4.2 cm^{-1} with a grating groove density of 900 lines/mm was used. Spectra were recorded at room temperature with a laser power of 500 mW, and a spectral resolution of 6 cm^{-1}. Each spectrum was obtained after collecting and averaging 1000 scans in order to obtain spectra with high signal-to-noise ratio. FT-Raman spectra were plotted as intensity (arbitrary units) against Raman shift in wavenumber units (cm^{-1}). All spectra were vector normalized in the whole range (4000–500 cm^{-1}). In order to improve signal-to-noise ratio in FTIR and Raman spectra, Tris–HCl buffer, BSA solutions and phen, Cu–phen and Cu–Met–phen solutions were lyophilized. Solutions were prepared in the same experimental conditions as fluorescence spectroscopy studies. As with other proteins, particularly globulins, FT-Raman spectra of protein solutions and freeze-dried powders are almost identical, therefore, freeze drying does not affect protein conformation. This behavior was taken into account during the experimental procedure. The plotting, processing, normalizations, manipulations, and evaluation of FT-IR and Raman spectra (band intensities, baseline corrections, normalization, derivation, curve fitting and area calculation) were carried out by means of Grams/32 (Galactic Industries Corporation, USA) software, OPUS 3.1 (Bruker Optics, Germany) and Perkin-Elmer software. Determination of intensity values for the typical tyrosine doublet and determination of secondary structure of BSA for the samples containing phen, Cu–phen and Cu–Met–phen solutions in BSA were carried out on the basis of the preceding described procedure [24] and according to that described by Byler and Susi [26]. All analyses were performed in three independent experiments, and the results were reported as averages of these replicates. A Bruker ESP300 spectrometer operating at X and Q-bands, and equipped with standard Oxford low temperature devices was used to record the EPR spectra of the compounds at different temperatures. The magnetic field was measured with a Bruker BNM 200 gaussmeter, and the frequency inside the cavity was determined by using a Hewlett–Packard 5352B microwave frequency counter. Anisotropic X-band EPR spectra of frozen solutions were recorded at 140 K, after addition of 10% ethylene glycol to ensure good glass formation. A computer simulation of the EPR spectra was performed using SimFonia software [5]. The concentration ratios were the same than those used in the fluorescence measurements.

The solutions (0.50 mM of the compounds: 2% w/v BSA) were also assayed by UV–vis electronic spectroscopy. Electronic absorption spectra were recorded with a Hewlett–Packard 8453 diode-array spectrophotometer, using 1 cm quartz cells in the 200–800 nm range. Buffer solutions were placed in the reference compartment. Three independent replicates of BSA solution and the corresponding complexes were measured.

3. Results and discussion

3.1. Acid phosphatase inhibiton test

Nowadays, enzyme inhibition through metal coordination action has widely reported associated to several pathologies [1,3]. For instance, vanadium coordination compounds are well recognized as phosphatase inhibitors [2] as well as their behavior as potent catalyst. Related to copper(II) complexes there are some studies associated to the inhibition of topoisomerase II catalytic activity [27]. Metal based complexes as inhibitors of PTP (protein tyrosine phosphatases) are also documented including copper(II) compounds [2]. Among a few examples found in the literature [28], in our ongoing search for new metal-based chemotherapeutic agents we began to study the inhibition on ALP provoked by copper(II) complexes [2]. But there are no so much examples related to metal(II) coordination compounds inhibiting AcP [18]. For this reason and the above mentioned seems to be the great interest to measure this effect for copper(II) complexes.

In order to evaluate the inhibition availability of the copper(II) ternary complex, free ligands (methimazole and phenanthroline) and binary complexes as Cu–phen and Cu–Met were also assessed. On the contrary to that observed on ALP, none of the free ligands presented inhibitory effect on AcP. In a previous work we demonstrated that methimazole behaved as a moderate inhibitor [5]. On the other hand, the chelating effect of phenanthroline producing

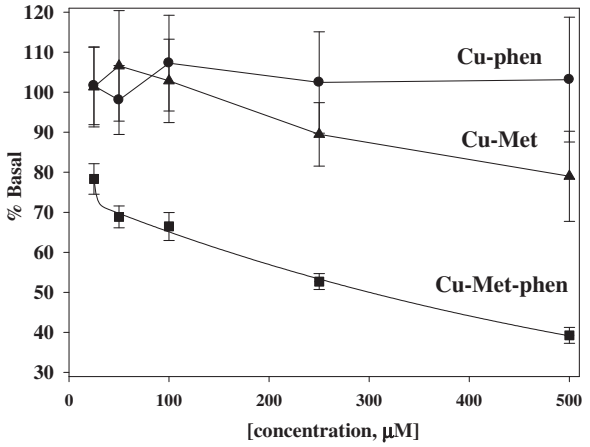

Fig. 2. Effect of copper(II) complexes on AcP activity. Cu–phen (filled circle), Cu–Met (filled triangle) and Cu–Met–phen (filled square). Initial rate was determined by incubation of the enzyme at 37 °C for 20 min in the absence or presence of variable concentrations of the inhibitors.

inhibition by the removal of Zn(II) from the ALP enzyme is well known [29].

In Fig. 2 the effects of copper(II) complexes on the AcP activity can be observed. As it can be seen, Cu–phen has not effect while Cu–Met produces a weak inhibition process that reaches a maximum of approximately a 20 percent of inhibition at a concentration of 500 μM. Surprisingly, the complexation of Cu(II) with both ligands in the Cu–Met–phen complex, clearly produces a metal-drug synergic behavior improving the inhibitory ability on AcP. At a concentration of 300 μM (0.163 mg/L), the complex inhibited a 50 percent the enzyme activity (IC_{50} value) being more effective than the vanadium complexes (Concentration ratio of 1 enzyme to 1000 complex exhibited some degree of inhibition) [18] and than the Cu(II) ion which presented inhibition at 0.7–100 mg/L concentration [14]. Up to now, for a first time the inhibition on AcP has been tested for a Cu(II) coordination complex and the inhibitory effect found for the enzymatic activity resulted in a great and potential field of applications for this new compound.

3.2. Anti-thyroid activity

A variety of oxygen, nitrogen and sulfur containing molecules having electron-donating groups in their chemical structure may have anti-thyroid activity [30]. This effect can be produced by: (i) complexation of molecular iodine in the thyroid gland, and (ii) through the inhibition of thyroid peroxidase enzyme (TPO). Both, iodine and TPO are involved in the synthesis of thyroid hormones (Fig. 3), iodine ion is oxidized by peroxidase to give iodonium ion, which iodinates tyrosine. The coupling reaction of L-mono-iodotyrosine (MIT) with L-di-iodo-tyrosine (DIT) affords L-tri-iodo-thyronine (T_3) and L-tetra-iodothyronine or thyroxine (T_4). Related to complexation with molecular iodine, it has been well established that iodine yields 1:1 molecular complexes with a variety of compounds [31]. In this context, methimazole was studied for several authors because of the interest in the study of thyroid diseases. The charge-transfer complex formation between methimazole and iodine in CH_2Cl_2 was studied by Freeman et al. [32] in CCl_4 forming a solid complex, Raby et al. [33] (K_c = 23.194 M^{-1}, 20 °C) and by Rousseau et al. [34] (K_c = 23.194 M^{-1}) (Table 1). In addition to the formation of stable transfer complexes with S-donor molecules, it has also been proven that complexation might occur at the nitrogen atoms of molecules containing purine ring group [22]. In our complexes the thioamide group is blocked due to metal-coordination but the ligand presented a free NH group and

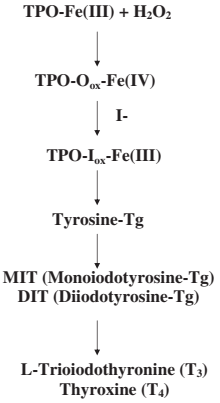

Fig. 3. Schematic representation of the formation of L-triiodothyronine (T_3) and thyroxine (T_4).

Table 1
Formation constant (K_c) of iodine charge transfer complexes.

Compound	K_c (M^{-1})	Solvent	Refs.
Methimazole	23,194	CCl_4	[33,35]
	27,096	CCl_4	[33]
	26,805	CCl_4	This work
	106,905	CH_2Cl_2	[35]
	41556.5	H_2O:CH_3–CH_2OH (1:1)	This work
Cu–Met	9538	H_2O:CH_3–CH_2OH (1:1)	This work
Cu–Met–phen	1.02×10^{10}	H_2O:CH_3–CH_2OH (1:1)	This work

this is the reason that we decided to test the anti-thyroid activities of the coordination complexes [5,6].

The charge–transfer complex formation can be easily detected by the appearance of a new band, the charge transfer (CT) band, which increases in intensity with the concentration of the complex or it can also be detected by the hypsochromic shift of the iodine band [30]. In our experimental conditions a blue shift of the free iodine band together with a remarkable increment in the intensity, is observed for methimazole, Cu–Met and Cu–Met–phen complexes after the interaction with iodine (Fig. 4, left). It has been proposed that the observed blue shift of the free iodine band upon complexation could be attributed to a perturbation of the iodine molecular orbital (σ^*) by a repulsive interaction between the iodine molecule in the CT complexes [20].

It is worthy to mention that the methimazole (not shown) and the copper(II)–methimazole complexes (Fig. 4, left, short dash line, as an example) have no absorption in the wavelength range that could perturb the corresponding new band. Maintenance of the typical d–d band for Cu(II) complexes let us to assume that there are no redox processes involved under our experimental conditions.

The method of Lang (Fig. 4, right) was thus employed to calculate the formation constant K_c (Table 1). It is well known that anti-thyroid activity can be expected for compounds whose K_c exceeds 100 M^{-1}. We first determined K_c for methimazole using CCl_4 as solvent (Table 1) being the calculated value close to previous reported data [33,35]. Because of the insolubility of the complexes in CCl_4, CH_2Cl_2 and other solvents, we determined K_c in a water–ethanol medium. The obtained K_c values are shown in Table 1. As it was expected for more polar solvents (water–ethanol), K_c value for methimazole is greater than that obtained in CCl_4 and CH_2Cl_2, showing a fairly good anti-thyroid activity [35]. Phenanthroline ligand was also tested showing no activity. Surprisingly, the copper(II) complexes presented also good activity, in particular Cu–Met–phen being 10^6 times more active than methimazole.

In general methimazole anti-thyroid activity was attributed to the thione–iodine interaction and several conformations (planar

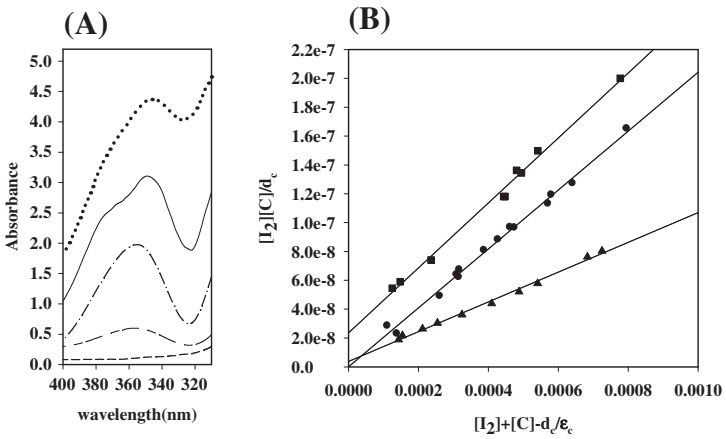

Fig. 4. (A) Electronic absorption spectra in the 310–400 nm region for Cu–Met–phen without iodine (4×10^{-4} M, short dash line), I_2 (4×10^{-4} M, short-long dash line), I_2–methimazole (4×10^{-4} M:4×10^{-4} M, dotted line), I_2–Cu–Met (4×10^{-4} M:4×10^{-4} M, solid line) and I_2–Cu–Met–phen (4×10^{-4} M:4×10^{-4} M, dash-dot-dash line); 298 K, ethanol–water 1:1 solutions, 1 cm of optical path length. Blue shift of the I_2 band appears around 354–345 nm. (B) Langs method: relationship between $[I_2][Ser]/d_c$ and $[I_2] + [Ser] - d_c/\varepsilon_c$ for I_2–methimazole (▲), I_2–Cu–Met (■) and I_2–Cu–Met–phen (●) complexes, concentration range: I_2 4×10^{-4} M, fixed, compounds: 7×10^{-4} M–0.5×10^{-4} M. The reaction was carried out directly in the spectrophotometric cell by mixing 1.5 mL solutions of each donor compounds and the acceptor (iodine).

and perpendicular) complexes have been proposed [34]. For the copper(II) complexes the thione moiety is blocked due the coordination with the metal center forming $Cu(II)S_2O_2$ and $Cu(II)S_2N_2$ coordination (equatorial plane) in Cu–Met and Cu–Met–phen complexes, respectively. In both, the coordination mode is retained in solution [5,6]. Then, it is possible to assume that the activity of the complexes comes from the non coordinated NH group belonging to methimazole molecule. The charge transfer complex formation of this type of molecules having NH group have been earlier demonstrated for 2-methylfuram [36], sertraline [22] and tricyclic antidepressants [34], among others. On the other hand, the difference in the anti-thyroid activity of the ternary complex could be related to the electron-donating effect of the system phenanthroline–copper that increases the basicity of the nitrogen atom of methimazol [37].

3.3. Antifungal activity and post-antifungal effect (PAFE) measurements

3.3.1. Antifungal activity

Metal based drugs represent a novel group of antifungal agents with potential applications for the control of fungal infections. Besides others, copper(II) complexes are usually investigated because their antifungal activity [38]. On the other hand, phenanthroline (phen) and its derivatives are well known since their effect on disturb the functioning of a wide variety of biological systems [39]. Also, they act as potential anti-tumor agents that could exert better anti-tumor activity if their hydrophilic groups are masked by copper ions to form water-soluble neutral complexes [40]. Phen derivatives are of interest due to their established activities against cancer, viral, bacterial, and fungal infections [41].

In a previous work we reported the antibacterial properties of the ternary Cu–Met–phen complex [6]. As part of continuous research on these complexes, the metal, the ligands and the complex were tested to determine the possible improvement of the antifungal activity upon complexation.

Taking into account that the tested complexes behaved as AcP inhibitors, considering that some acid phosphatase enzymes are extracted from some fungi strains (including *C. albicans*) [42], we consider of relevance to determine the activity of these compounds as potential antifungal agents.

Nevertheless, MIC values are important experimental data in antimicrobial assay to determine the susceptibility of some microorganisms against antimicrobial agents it provides limited information on the activity of the drug in the course of time. In this context, the determination of the post-antibiotic effect (PAE) and the post-antifungal effect (PAFE) of antibacterial and antifungal drugs is very important nowadays. The concepts about the PAE are also applicable to the PAFE. The PAE is a persistent suppression of bacterial growth following short antibiotic exposure. The PAE/PAFE is a pharmacodynamic parameter and the presence of this effect may be an important consideration in designing antibiotic dosage regimens. Determination of the PAE/PAFE is recommended in pre-clinical evaluation of all new antimicrobial/antifungal agents because it is a determinant factor that affects optimal antimicrobial dosing intervals [43]. In the present study, the PAFEs of the active copper complexes for the three strains of Candida were studied.

The results of the antifungal activity assays are given in Table 2. It is well documented that *in vitro* measurements MIC values greater than 1000 μg mL^{-1} are considered with no relevance from a clinical perspective [5]. In this context, the antifungal activity of the $CuCl_2{\cdot}2H_2O$, methimazole, Cu–Met and Cu–Met–phen against all tested strains are considered not significantly relevant. Nevertheless, the free ligand phen and the complex Cu–phen show good antifungal activity against all strains of Candida. As we have previously reported, the free ligand phen was the most active antifungal compound tested on *C. albicans* showing the lowest MIC values [23]. No improvement in this activity of the non-active methimazole is produced by its complexation with Cu(II) in contrast with the antibacterial one. Like the antibacterial activity of this metal, the antifungal activity of copper was enhanced by complexation. Some MIC values of copper(II) ion against different fungal strains were previously reported being in accordance with our results [5,41]. Besides, our results on the MIC values of phen against

Table 2
Minimum inhibitory concentration (MIC) of $CuCl_2{\cdot}2H_2O$, the free ligands (phen and Met), and the copper(II) complexes for the fungal strains (μg mL^{-1}).

	C. albicans	*C. tropicalis*	*C. parapsilosis*
$CuCl_2{\cdot}2H_2O$[a]	>1500	>1500	>1500
o-Phenanthroline[a]	3.00	12.00	12.00
Methimazole	1500	>1500	>1500
Cu–Met	1500	1500	1500
Cu–phen	11.71	46.87	46.87
Cu–Met–phen	1500	1500	1500
Fluconazole[a]	>375	1.5	6

[a] Data from Ref. [37].

different strains of Candida agree with those reported by Creaven et al. [44] (MIC = 3.31 μg mL^{-1}).

The antifungal activity information related to ternary copper(II)-L-phen (L = different kind of ligands) complexes referred usually to the effect on *C. albicans* [45–47]. For Cu(II)–dicoumarol–phen complexes only one of the complexes named as *HPC3* presented a MIC value on *C. albicans* (ATCC66027) the half of that of the ligand alone but there were no comparisons with the effect produced by isolate phen [28]. Copper(I)-L-phen complexes were also proved against *C. albicans* (from clinical samples). [CuI(2,2-biquinoline)$P(CH_2N(CH_2CH_2)_2O)_3$] complex showed a MIC value of 100 μg mL^{-1} while for Cu(I) iodide complexes with aminomethyl phosphanes were in the 80–160 μg mL^{-1} range. In any case the MIC values were better than those obtained for Cu–phen [48,49]. Antifungal activity of Cu–phen complexes ($Cu(phen)^{2+}$, $Cu(phen)_2^{2+}$) were also checked, but no specific data for these complexes were found. For this reason our data seems to be relevant confirming the tendency of the improvement of the biological behavior of the metal mediated by the ligand.

3.3.2. Post-antifungal effect (PAFE) measurements

The PAFE is usually defined as the period of inhibition of fungal growth after the antifungal has been completely removed. This period can also be a measure of the delayed regrowth of fungi after a short period of antifungal exposure [23]. A zero value was assigned to PAFEs values of 20 min or less since it was considered not significant. The PAFEs of the $CuCl_2{\cdot}2H_2O$, methimazole, Cu–Met and Cu–Met–phen were not determined because these compounds exert no activity against fungal strain (MIC > 1500 μg mL^{-1}). The ligand phen exhibited no PAFEs against the tree strains of Candida (PAFE < 20 min).

The complex Cu–phen exhibited a longer PAFE against *C. parapsilosis* (2.92 ± 0.25 h) than for *C. albicans* (0.44 ± 0.05 h). Nevertheless, this complex exhibited no PAFEs against *C. tropicalis*. The enhanced PAFE values upon complexation can be explained on the bases of Tweedy's chelation theory. On this theory, chelation reduces the polarity of the central metal atom because of partial sharing of its positive charge with the ligand. Further, it increases the delocalization of π-electrons over whole chelate ring and enhances lipophilicity of the complexes [5]. This increment in the lipophilicity of the Cu–phen complex could be responsible for the longer PAFEs on fungal strains because the complex could remain more time in the lipid bilayer. However, the lack of this effect against *C. tropicalis* can't be explained by this theory. From a clinical point of view, the increment of PAFE values upon complexation with copper(II) is taken into consideration in the design of antibiotic dosage regimens allowing the extension of antifungal dosing intervals beyond the time that antifungal concentrations fall below the MIC.

PAE/PAFE reports are not usually evaluated for metal complexes. Our research group began to evaluate PAE/PAFE as a complementary data [23]. The PAFEs of the complex Cu–phen were compared with the PAFEs reported in the literature for some antifungal agents (similar experimental conditions and fungal strains).

While the MIC values corresponding to *C. parapsilosis* and *C. albicans* were similar to that found for [Cu(phen)(cnge)$(H_2O)(NO_3)_2$] complex (cnge = cyanoguanidine) [23], in both cases the PAFEs values were higher than the Cu–phen complex.

4. Interaction of the metal complex with bovine serum albumin

4.1. Binding affinity of the metal complex with bovine serum albumin

The aim of this section is to determine the affinity of the Cu–Me–phen complex to bovine serum albumin (BSA) which has usually been used as a model. In a previous work we studied the interaction with BSA for Cu–Met complex. In this work, the interaction of the phen ligand and Cu–phen complex were included for comparative purposes.

It is well know that albumin binds to a variety of substrates, including metal cations, fatty acids, amino acids, hormones and several therapeutic drugs. It has been shown that the distribution, the free concentration and the metabolism of various drugs can be significantly altered as a result of their bindings to BSA. This binding ability could be evaluated using fluorescence spectroscopy.

The fluorescence quenching is the procedure that could weaken the fluorescence intensity of a fluorescent compound through several processes. The intrinsic fluorescence of BSA comes from the tryptophan and tyrosyl amino acid residues of its structure. The changes of fluorescence or absorption spectra of BSA reflect the interaction of the drugs with the macromolecular protein. Several drugs and other bioactive small molecules bind reversibly to albumin and typical association constants (K_a) values from 10^4 to 10^6 M^{-1} indicated a carrier behavior. Serum albumin often increases the apparent solubility of hydrophobic drugs in plasma and modulates their delivery to cell *in vivo* and *in vitro*.

In our experiments, the fluorescence intensity of BSA was affected showing a significant decrease and the band was moved to higher wavelengths values (red-shift) of the maximum emission wavelength (Fig. S1). This change implies that the conformation of BSA is changed and the tryptophan and tyrosine residues are located in a less hydrophobic environment [24,25]. To determine the type of fluorescence quenching, the Stern–Volmer equation was applied (calculated curves can be seen in Fig. S2 in which, a linear dependence was established). The K_{sv} constants at 25 °C were calculated giving a final value of 41.70×10^3 M^{-1} for phen–BSA, 26.77×10^3 M^{-1} for Cu–phen–BSA and 44.10×10^3 M^{-1} for Cu–Met–phen–BSA. Based in the relationship $K_q = K_{sv}/\tau_0$ (where τ_0 is the average lifetime of the biomolecule without quencher), the dynamic quenching constant K_q has also been calculated giving values of 41.70×10^{11} M^{-1} s^{-1}, 26.77×10^{11} M^{-1} s^{-1} and 44.10×10^{11} M^{-1} s^{-1}, respectively. These constants were greater than $K_{q(max)}$ (2×10^{10} M^{-1} s^{-1}, reference value) meaning that for these complexes the quenching is not initiated by dynamic collision, but it could possible be originated from the interaction of the ligand or the complex with the albumin [25]. A different mechanism was determined for the interaction of the Cu–phen complex with BSA. The graph lines of the Fig. S2 is bent upward, so the Stern–Volmer equation has only been used in the linear range (Fig. S2, inset). The calculated K_{sv} values are indicative that the formation of the ternary complex clearly improves the interaction with the albumin since it is greater than that of the binary complex Cu–phen.

The apparent static binding constant (K_a) and the number of binding sites, *n* value, were calculated for Cu–Met–phen complex. The K_a value (4.820×10^5 M^{-1}) point to a reversible binding of the complex to albumin and the "*n*" value (1.33) mean that there was one independent class of binding site on the albumin for complex. Therefore, it can be assumed that this complex may be stable in biological systems and may be carried by albumin.

4.2. Conformational changes induced on BSA structure

Because: (i) there is evidence of conformational changes in BSA after interaction with low molecular weight ligands and (ii) it is well known that these changes affect the secondary and tertiary structure of albumin, these molecular interactions were monitored by spectroscopic techniques (FT-IR, Raman, UV–vis).

The tertiary structure of BSA was analyzed by the changes produced on the vibrations of the side chain (tyrosine and tryptophan modes) and disulfide region. The Secondary structure was studied exploring typical Amide I protein band. Then, these results were

correlated with the changes observed in the typical UV–vis bands of the albumin.

In the Raman spectra, the ratio of the tyrosyl doublet at 850 and 830 cm^{-1} has been used to determine whether the tyrosine residues in proteins are exposed or buried [5]. After the addition of phen, Cu–phen and Cu–Met–phen solutions, a significant modification in the tyrosine doublet of BSA was observed indicating that the microenvironments of tyrosyl groups were greatly altered by the interaction with the compounds. Fig. 5 (top panel) shows the calculated $I_{850/830}$ ratio for each compound. For the ternary complex there is a decrease in the $I_{850/830}$ ratio suggesting that tyrosine residue formed a more buried environment in comparison with BSA indicating an involvement of tyrosyl residues in the inter or intramolecular interactions. In the phenanthroline samples there is an increment in this ratio meaning a change of the tyrosyl residues from middle to a more exposed environment. On the other hand, the absence of a definite peak at *ca.* 1360 cm^{-1} (indicative of buried tryptophan residues) suggests that the tryptophan rich domain is partly accessible being exposed and available to interact [24]. This result is coincident to the observed red-shift in the fluorescence spectra suggesting the unfolding of the protein. In addition, the opening of the structure of the BSA was accompanied by modifications in the S–S disulfide region (500–550 cm^{-1} region). It is established that the position of these bands are sensitive to the conformation of the C–C–S–S–C–C sequence. Bands at *ca.* 510, 525, and 540 cm^{-1} are characteristic of the *gauche–gauche–gauche (g–g–g)*, *gauche–gauche–trans (g–g–t)*, and *trans–gauche–trans (t–g–t)* conformation of the C–C–S–S–C–C sequence, respectively [24]. The modifications of intensity in these bands are shown in Fig. 5 (bottom panel). It was shown that in BSA the *g–g–t* configuration is higher than the *g–g–g* one while the *t–g–t* is less represented. The ligand phenanthroline and the Cu–phen complex caused a rearrangement of the S–S giving rise to an increment of the proportion of the configuration modes attributed to *t–g–t* and *g–g–t* conformations of the S–S disulfide bonds. On the other hand, the presence of copper(II) ion in the complexes provoked the splitting of the bands in the *t–g–t* region. The appearance of these two bands was suggested to be associated to the two types of S–S configuration, intrachain and interchain disulfide bonds, in that order [24]. Apart this change, the most striking spectral change in the ternary complex was the disappearance of the band related to the *g–g–g* conformation revealing a strongest alteration in the disulfide bonds because of the loss in the local conformation of the most energetically stable one. This loss may be associated with the rupture of disulfide bridges of the *g–g–g* conformation due to unfolding of the protein.

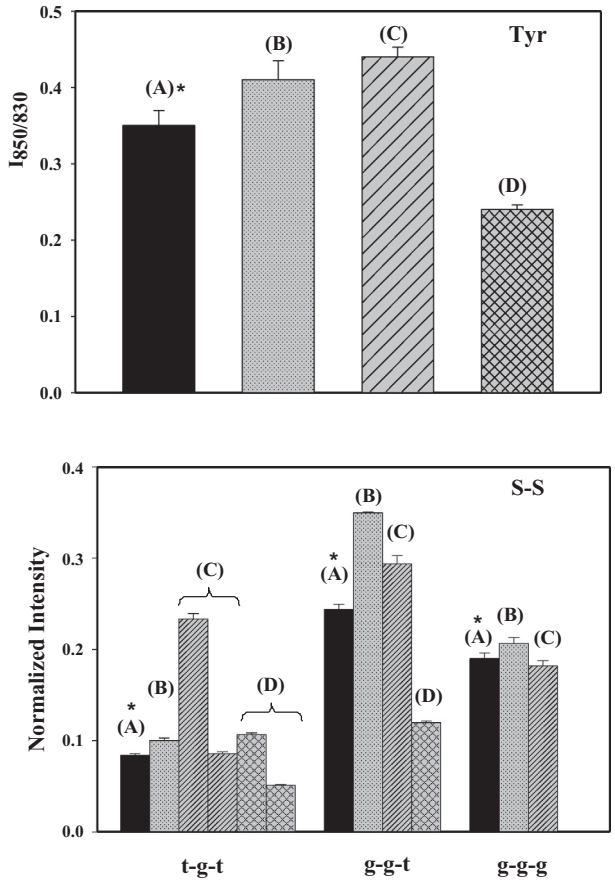

Fig. 5. Raman spectra. Top panel: $I_{850/830}$ ratio of (A) free BSA* (2% w/v) from Ref. [6], (B) phen–BSA (0.5 mM:2% w/v), (C) Cu–phen–BSA (0.5 mM:2% w/v), and (D) Cu–Met–phen–BSA (0.5 mM:2% w/v). Bottom panel: normalized intensity of the Raman S–S stretching vibrations in the 470–550 cm^{-1} region A–D references as described before.

In the FTIR spectra, amide I band (1700–1600 cm^{-1}, 70–85% of the νC=O stretching vibration mode) was taken into consideration. According to the curve fitting procedure, the area of each component and the type of secondary structure was calculated (Table S1). There was a decrease in α-helix conformation percentage relative to free BSA [26] being this effect higher for copper(II)-complexes especially in the ternary one. In this case, the strong reduction observed in α-helix conformation and the considerable enhancement in disordered structures in relation to BSA native structure suggested a strong interaction between copper(II)-complexes and BSA together with the unfolding of the protein and the losing of their majority α-helix conformation. Phenanthroline did not produce this strong effect on this conformation being reduced only in a 10% in comparison with free BSA. The structural modification leads mainly to the increment of percentage of the β-antiparallel component (disorder structures).

When the UV–vis spectra were also analyzed (Fig. S3), the absorption peaks of these solutions showed marked shifts toward shorter wavelengths with respect to the BSA blank indicating that as a consequence of the interaction the peptide strands of BSA the molecules were more extended. There is also a significant intensity increment in the bands that could be due to a higher exposure of aromatic amino acid residues [5]. This behavior is in concordance with the Raman measurements in which the exposition of the Trp residues was revealed.

Until now, we evaluated the degree of association and interaction of the complex with BSA. In order to know if it is stable in this simulated biological media and try to find which residues of the protein are probable interacting with the complex, we explore copper(II) ligand environment in Cu–Met–phen–BSA system (0.5 mM-2% w/v solution of Cu–Met–phen–BSA system) by EPR and UV–vis spectroscopies.

The electronic spectrum in the visible region displayed a typical broad band with maximum at 665 nm which is assigned to the d–d transitions of the copper(II) ion (450–830 nm region, rather asymmetric due to d^9 configuration Jahn–Teller effect). This band appears slightly shifted to longer wavelengths (red shift) in comparison to the spectrum of the complex in aqueous solution (λ = 658 nm) [6]. The EPR spectrum was recorded at 140 K (Fig. S4) in order to assist in the identification of the copper(II) species and the corresponding geometry, particularly the equatorial ligand donor set, and the overall charges involved in the BSA interactions. The simulation predicted the existence of unique solution species in which the EPR signal is originated by a Cu(II)-chromophore with the spin Hamiltonian parameters of $g_{\|} = 2.255$, $g_{\perp} = 2.090$ ($g_{\|} > g_{\perp} > 2.040$ consistent with a d^2_{x-y} ground state in an elongated octahedron) and the hyperfine coupling constant of $A_{\|} = 184 \times 10^{-4}$ cm^{-1}, $A_{\perp} = 15 \times 10^{-4}$ cm^{-1} ($g_{iso} = 2.145$, $A_{iso} = 71.3 \times 10^{-4}$ cm^{-1}). EPR parameters of the single

signal were consistent with data previously reported suggesting that the equatorial environment of copper(II) in Cu–Met–phen complex (CuN_2S_2) [5,6] is retained after albumin interaction. Assuming that the ligands remain coordinated to the metal in the interaction with BSA it is then possible to suggest that the contact takes place *via* Trp residues (van der Walls, H bond formation) which are exposed at the moment of the interaction, as demonstrated by Raman measurements.

5. Conclusions

As it was mentioned, there are few examples of metal coordination complexes as AcP inhibitors in which Cu(II) complexes are not included. In this work, we tested for a first time AcP inhibition mediated by the new Cu(II) methimazole complexes. It was evident that the presence of phenanthroline ligand in the coordination sphere of the metal center became relevant in the specific inhibitory effect on AcP. The octahedral coordination significantly improves the inhibition behavior in comparison with the very scarce effect produced for Cu–Met and the inactive methimazole. Anti-thyroid activity was also determined for a first time for metal complexes. In this experience, methimazole, Cu–Met y Cu–Met–phen behaved as anti-thyroid agents. It is remarkably that copper(II) complexation produced a metal-drug synergy behavior being this effect more significant in the ternary complex which was 10^6 times more active than methimazole.

By binding affinity measurements it was concluded that the complex interacted with BSA and might be carried by the protein (K_a, 10^4–10^6 M^{-1}). It was also established that the complex maintained its equatorial coordination sphere (EPR) after BSA interaction and that the mechanism of the interaction would be through Trp residues of the protein that became exposed after the opening of the BSA structure with a partial loss of the α-helix conformation (FTIR, Raman).

Conflict of Interest

The authors declare that there are no conflicts of interest.

Transparency Document

The Transparency document associated with this article can be found in the online version.

Acknowledgements

This work was supported by UNLP, UNCAUS, CONICET, CICPBA (No. 813/13) and ANPCyT (PICT-2013-0569), Argentina. EGF is a research fellow of CONICET. PAMW is a research fellow of CICPBA, Argentina. MSI, MJL and JJMM are fellowship holders from CONICET.

Appendix A. Supplementary data

Supplementary data associated with this article can be found, in the online version, at http://dx.doi.org/10.1016/j.cbi.2014.12.036.

References

[1] C.-M. Che, F.-M. Siu, Metal complexes in medicine with a focus on Enzyme Inhibition, Curr. Opin. Chem. Biol. 14 (2010) 255–261.
[2] L. Lu, M. Zhu, Metal-based inhibitors of protein tyrosine phosphatases, Anti-Cancer Agents Med. Chem. 11 (2011) 164–171.
[3] A.Y. Louie, T.J. Meade, Metal complexes as enzyme inhibitors, Chem. Rev. 99 (1999) 2711–2734.
[4] Y. Li, L. Lu, M. Zhu, Q. Wang, C. Yuan, S. Xing, X. Fu, Y. Mei, Potent inhibition of protein tyrosine phosphatases by copper complexes with multi-benzimidazole derivatives, BioMetals 24 (2011) 993–1004.
[5] N.M. Urquiza, S.G. Manca, M.A. Moyano, R. Arrieta Dellmans, L. Lezama, T. Rojo, L.G. Naso, P.A.M. Williams, E.G. Ferrer, Copper(II) complexes of methimazole, an anti Grave's disease drug. Synthesis, characterization and its potential biological behavior as alkaline phosphatase inhibitor, BioMetals 23 (2010) 255–264.
[6] N.M. Urquiza, M.S. Islas, M.L. Dittler, M.A. Moyano, S.G. Manca, L. Lezama, T. Rojo, J.J. Martínez Medina, M. Diez, L. López Tévez, P.A.M. Williams, E.G. Ferrer, Inhibition behavior on alkaline phosphatase activity, antibacterial and antioxidant activities of ternary methimazole–phenanthroline–copper(II) complex, Inorg. Chim. Acta 405 (2013) 243–251 (and references therein).
[7] D.L. Wang, R.C. Holz, S.S. David, L. Jr, That, M.T. Stankovich, electrochemical properties of the diiron core of uteroferrin and its anion complexes, Biochemistry 30 (1991) 8187–8194.
[8] P.V. Bernhardt, G. Schenk, G.J. Wilson, Direct electrochemistry of porcine purple acid phosphatase (uteroferrin), Biochemistry 43 (2004) 10387–10392.
[9] E. Ouija, M. Soberon, H. Haak-Mares, Mechanism of action of acid phosphatases of low molecular weight, An. Medic. Fac. Lima 68 (2007) 356–362.
[10] D. Feder, W.M. Hussein, D.J. Clayton, M.-W. Kan, G. Schenk, R.P. McGeary, L.W. Guddat, Identification of purple acid phosphatase inhibitors by fragment-based screening: promising new leads for osteoporosis therapeutics, Chem. Biol. Drug Des. 80 (2012) 665–674.
[11] C. Ozu, J. Nakashima, Y. Horiguchi, M. Oya, T. Ohigashi, M. Murai, Prediction of bone metastases by combination of tartrate-resistant acid phosphatase, alkaline phosphatase and prostate specific antigen in patients with prostate cancer, Int. J. Urol. 15 (2008) 419–422.
[12] A. Taira, G. Merrick, K. Wallner, M. Dattoli, Reviving the acid phosphatase test for prostate cancer, Oncology 21 (2007) 1003–1010.
[13] D. Olczak-Kowalczyk, A. Witt, D. Gozdowski, M. Ginalska-Malinowska, Oral mucosa in children with Prader–Willi syndrome, J. Oral Pathol. Med. 40 (2011) 778–784.
[14] U. Blum, G. Schwedt, Inhibition behavior of acid phosphatase and adenosine deaminase phosphodiesterase I as trace metal analysis tools and speciation, Anal. Chim. Acta 360 (1998) 101–108.
[15] M. Vlahović, L. Ilijin, A. Matic, J. Lazarević, V. Nenadović, V. Perić-Mataruga, M. Mrdaković, Cadmium effects on the ratio of activities of lysosomal acid phosphatases and Total (ACPLys/ACPTot) in Lymantria dispar larvae, Arch. Biol. Sci. 65 (2013) 345–352.
[16] N.G. Juma, M.A. Tabatabai, Effects of trace elements on phosphatase activity in soils, Soil Sci. Soc. Am. J. 41 (1977) 343–346.
[17] S.H. Mohd-Pahmi, W.M. Hussein, G. Schenk, R.P. McGeary, Synthesis, modeling and kinetic assays of potent inhibitors of purple acid phosphatase, Bioorg. Med. Chem. Lett. 21 (2011) 3092–3094.
[18] C.C. McLauchlan, J.D. Hooker, M.A. Jones, Z. Dymon, E.A. Backhus, B.A. Greiner, N.A. Dorner, M.A. Youkhana, L.M. Manus, Inhibition of acid, alkaline and tyrosine (PTP1B) phosphatases by novel vanadium complexes, J. Inorg. Biochem. 104 (2010) 274–281.
[19] D.S. Cooper, Antithyroid drugs, N. Engl. J. Med. 352 (2005) 905–917.
[20] U.M. Rabie, M.H.M. Abou-El-Wafa, H. Nassar, In vitro simulation of the chemical scenario of the action of an anti-thyroid drug: charge transfer interaction of thiazolidine-2-thione with iodine, Spectrochim. Acta Part A 78 (2011) 512–517.
[21] F. Isaia, M.C. Aragoni, M. Arca, F. Demartin, F.A. Devillanova, G. Floris, A. Garau, G. Verani, Interaction of methimazole with I_2: X-ray crystal structure of the charge transfer complex methimazole–I_2. Implications for the mechanism of action of methimazole-based antithyroid drugs, J. Med. Chem. 51 (2008) 4050–4053.
[22] G.E. Escudero, V. Ferraresi Curotto, C.H. Laino, R. Pis Diez, P.A.M. Williams, E.G. Ferrer, Sertraline and its iodine product: experimental and theoretical vibrational studies. Potential *in vitro* anti-thyroid activity of sertraline and iodine product toxicity with respect to male Wistar rats, Spectrochim. Acta Part A 104 (2013) 271–279.
[23] J.J. Martínez Medina, M.S. Islas, L.L. López Tévez, E.G. Ferrer, N.B. Okulik, P.A.M. Williams, Copper(II) complexes with cyanoguanidine and o-phenanthroline: theoretical studies, in vitro antimicrobial activity and alkaline phosphatase inhibitory effect, J. Mol. Struct. 1058 (2014) 298–307.
[24] N.M. Urquiza, L.G. Naso, S.G. Manca, L. Lezama, T. Rojo, P.A.M. Williams, E.G. Ferrer, Antioxidant activity of methimazole–copper(II) bioactive species and spectroscopic investigations on the mechanism of its interaction with Bovine Serum Albumin, Polyhedron 31 (2012) 530–538.
[25] J.R. Lakowicz, Principles of Fluorescence Spectroscopy, 2nd ed., Plenum Press, New York, 1999. p. 237.
[26] D.M. Byler, H. Susi, Examination of the secondary structure of proteins by deconvolved FTIR spectra, Biopolymers 25 (1986) 469–487.
[27] D. Jayaraju, A.K. Kondapi, Anti-cancer copper salicylaldoxime complex inhibits topoisomerase II catalytic activity, Curr. Sci. 81 (2001) 787–792.
[28] C.J. Martin, W.J. Evans, Reversible inhibition of intestinal alkaline phosphatase by inositol hexaphosphate and its Cu(II) coordinate complexes, J. Inorg. Biochem. 15 (1991) 177–178.
[29] D. Plocke, B. Vallee, Interaction of alkaline phosphatase of *E. coli* with metal ions and chelating agents, Biochemistry 1 (1962) 1039–1043.
[30] M. Esseffar, W. Bouab, A. Lamsabhi, J.-L.M. Abboud, R. Notario, M. Yáñez, An experimental and theoretical study on some thiocarbonyl–I_2 molecular complexes, J. Am. Chem. Soc. 122 (2000) 2300–2308.

[31] G.J. Corban, S.K. Hadjikakou, N. Hadjiliadis, M. Kubicki, E.R.T. Tiekink, I.S. Butler, E. Drougas, A.M. Kosmas, Synthesis, structural characterization, and computational studies of novel diiodine adducts with the heterocyclic thioamides N-methylbenzothiazole-2-thione and benzimidazole-2-thione: implications with the mechanism of action of antithyroid drugs, Inorg. Chem. 44 (2005) 8617–8627.
[32] F. Freeman, J.W. Ziller, H.N. Po, M.C. Keindl, Reactions of imidazole-2-thiones with molecular iodine and the structures of two crystalline modifications of the 1:1 1,3-dimethylimidazole-2-thione-diiodine charge–transfer complex ($C_5H_8I_2N_2S$), J. Am. Chem. Soc. 110 (1988) 2586–2591.
[33] C. Raby, J.F. Lagorce, A.C. Jambut-Absil, J. Buxeraud, G. Catanzano, The mechanism of action of synthetic antithyroid drugs: iodine complexation during oxidation of iodide, Endocrinology 126 (1990) 1683–1691.
[34] A. Rousseau, F. Comby, J. Buxeraud, C. Raby, Spectroscopic analysis of charge transfer complex formation and peroxidase inhibition with trycyclic antidepressant drugs: potential anti-thyroid action, Biol. Pharm. Bull. 19 (1996) 726–728.
[35] C. Laurence, M.J. El Ghomari, J.-Y. Le Questel, M. Berthelot, R. Mokhlisse, Structure and molecular interactions of anti-thyroid drugs. Part 3.1: methimazole: a diiodine sponge, J. Chem. Soc. Perkin Trans. 2 (1998) 1545–1551.
[36] R.P. Lang, Molecular complexes and their spectra. XV. Iodine complexes with thiophene, 2-methylfuran and N-methylpyrrole, J. Am. Chem. Soc. 84 (1962) 4438–4441.
[37] M.J. El Ghomari, R. Mokhlisse, C. Laurence, J.-Y. Le questel, M. Berthelot, Basicity of azoles: complexes of diiodine with imidazoles, pyrazoles and triazoles, J. Phys. Org. Chem. 10 (1997) 669–674.
[38] H.R. Dholariya, K.S. Patel, J.C. Patel, A.K. Patel, K.D. Patel, Thermal, kinetic, spectroscopic studies and anti-microbial, antituberculosis, anti-oxidant properties of clioquinol and benzocoumarin derivatives mixed complexes with copper ion, Med. Chem. Res. 22 (2013) 5848–5860.
[39] S. Chandraleka, K. Ramya, G. Chandramohan, D. Dhanasekaran, A. Priyadharshini, A. Panneerselvam, Antimicrobial mechanism of copper (II) 1,10-phenanthroline and 2,2-bipyridyl complex on bacterial and fungal pathogens, J. Saudi Chem. Soc. (2011), http://dxdoi.org/10.1016/j.jscs.2011.11.020.
[40] R.N. Patel, N. Singh, K.K. Shukla, J. Niclós-Gutiérrez, A. Castineiras, V.G. Vaidyanathan, B. Unni Nair, Characterization and biological activities of two copper(II) complexes with diethylenetriamine and 2,2′-bipyridine or 1,10-phenanthroline as ligands, Spectrochim. Acta Part A 62 (2005) 261–268.
[41] S. Roy, K.D. Hagen, P.U. Maheswari, M. Lutz, A.L. Spek, J. Reedijk, G.P. van Wezel, Phenanthroline derivatives with improved selectivity as DNA-targeting anticancer or antimicrobial drugs, Chem. Med. Chem. 3 (2008) 1427–1434.
[42] E. Vasileva-Tonkodvaan, K. Galabovam, A. Balasheva, A.V. Sotirova, Purification and partial characterization of acid phosphatase from *Candida lipolytica*, J. Gen. Microbiol. 139 (1993) 419–483.
[43] W.J. Stubbings, J.M. Bostock, E. Ingham, I. Chopra, Assessment of a microplate method for determining the post-antibiotic effect in *Staphylococcus aureus* and *Escherichia coli*, J. Antimicrob. Chemother. 54 (2004) 139–143.
[44] B.S. Creaven, D.A. Egan, D. Karcz, K. Kavanagh, M. McCann, M. Mahon, A. Noble, B. Thati, M. Walsh, Synthesis, characterisation and antimicrobial activity of copper(II) and manganese(II) complexes of coumarin-6,7-dioxyacetic acid (cdoaH2) and 4-methylcoumarin-6,7-dioxyacetic acid (4-MecdoaH2): X-ray crystal structures of [Cu(cdoa)(phen)2].8.8H2O and [Cu(4-Mecdoa)(phen)2]13H2O (phen = 1,10-phenanthroline), J. Inorg. Biochem. 101 (2007) 1108–1119.
[45] H.R. Dholariya, K.S. Patel, J.C. Patel, K.D. Patel, Dicoumarol complexes of Cu(II) based on 1,10-phenanthroline: synthesis, X-ray diffraction studies, thermal behavior and biological evaluation, Spectrochim. Acta Part A 108 (2013) 319–328.
[46] T.S. Lobana, S. Indoria, A.K. Jassal, H. Kaur, D.S. Arora, J.P. Jasinski, Synthesis, structures, spectroscopy and antimicrobial properties of complexes of copper(II) with salicylaldehyde N-substituted thiosemicarbazones and 2,20-bipyridine or 1,10-phenanthroline, Eur. J. Med. Chem. 76 (2014) 145–154.
[47] N. Raman, R. Mahalakshmi, Bio active mixed ligand complexes of Cu(II), Ni(II) and Zn(II): synthesis, spectral, XRD, DNA binding and cleavage properties, Inorg. Chem. Commun. 40 (2014) 157–163.
[48] R. Starosta, K. Stokowa, M. Florek, J. Król, A. Chwiłkowska, J. Kulbacka, J. Saczko, J. Skała, M. Jeżowska-Bojczuk, Biological activity and structure dependent properties of cuprous iodide complexes with phenanthrolines and water soluble tris (aminomethyl) phosphanes, J. Inorg. Biochem. 105 (2011) 1102–1108.
[49] R. Starosta, A. Brzuszkiewicz, A. Bykowska, U.K. Komarnicka, B. Bazanów, M. Florek, L. Gadzała, N. Jackulak, J. Król, K. Marycz, A novel copper(I) complex, [CuI(2,2′-biquinoline)P($CH_2N(CH_2CH_2)2O)_3$] – synthesis, characterisation and comparative studies on biological activity, Polyhedron 50 (2013) 481–489.